

Multiple Mechanisms in Proton-Induced Nucleon Removal at ~ 100 MeV/Nucleon

T. Pohl,¹ Y. L. Sun,^{1,2,3,*} A. Obertelli,^{1,2} J. Lee,³ M. Gómez-Ramos,⁴ K. Ogata,^{5,6} K. Yoshida,⁷ B. S. Cai,⁸ C. X. Yuan,⁸ B. A. Brown,⁹ H. Baba,¹⁰ D. Beaumel,¹¹ A. Corsi,² J. Gao,^{10,12} J. Gibelin,¹³ A. Gillibert,² K. I. Hahn,^{14,15} T. Isobe,¹⁰ D. Kim,^{14,15} Y. Kondo,¹⁶ T. Kobayashi,¹⁷ Y. Kubota,^{10,18} P. Li,³ P. Liang,³ H. N. Liu,^{1,2,19} J. Liu,³ T. Lokotko,³ F. M. Marqués,¹³ Y. Matsuda,^{20,21} T. Motobayashi,¹⁰ T. Nakamura,¹⁶ N. A. Orr,¹³ H. Otsu,¹⁰ V. Panin,^{10,2} S. Y. Park,^{14,10} S. Sakaguchi,⁵ M. Sasano,¹⁰ H. Sato,¹⁰ H. Sakurai,^{10,22} Y. Shimizu,¹⁰ A. I. Stefanescu,^{23,24,10} L. Stuhl,^{10,15} D. Suzuki,¹⁰ Y. Togano,^{16,10,25} D. Tudor,^{23,24,10} T. Uesaka,¹⁰ H. Wang,¹⁰ X. Xu,³ Z. H. Yang,¹⁰ K. Yoneda,¹⁰ and J. Zenihiro¹⁰

¹*Institut für Kernphysik, Technische Universität Darmstadt, 64289 Darmstadt, Germany*

²*IRFU, CEA, Université Paris-Saclay, F-91191 Gif-sur-Yvette, France*

³*Department of Physics, The University of Hong Kong, Pokfulam, Hong Kong*

⁴*Departamento de Física Atómica, Molecular y Nuclear, Facultad de Física, Universidad de Sevilla, Apartado 1065, E-41080 Sevilla, Spain*

⁵*Department of Physics, Kyushu University, Fukuoka 812-8581, Japan*

⁶*Research Center for Nuclear Physics (RCNP), Osaka University, Ibaraki 567-0047, Japan*

⁷*Advanced Science Research Center, Japan Atomic Energy Agency, Tokai, Ibaraki 319-1195, Japan*

⁸*Sino-French Institute of Nuclear Engineering and Technology, Sun Yat-Sen University,*

Zhuhai, 519082 Guangdong, People's Republic of China

⁹*Department of Physics and Astronomy and the Facility for Rare Isotope Beams, Michigan State University,*

East Lansing, Michigan 48824-1321, USA

¹⁰*RIKEN Nishina Center, 2-1 Hirosawa, Wako, Saitama 351-0198, Japan*

¹¹*Université Paris-Saclay, CNRS/IN2P3, IJCLab, 91405 Orsay, France*

¹²*State Key Laboratory of Nuclear Physics and Technology, School of Physics, Peking University,*

Beijing 100871, People's Republic of China

¹³*LPC Caen, ENSICAEN, Université de Caen, CNRS/IN2P3, F-14050 Caen, France*

¹⁴*Department of Physics, Ewha Womans University, Seoul, South Korea*

¹⁵*Center for Exotic Nuclear Studies, Institute for Basic Science, Daejeon 34126, South Korea*

¹⁶*Department of Physics, Tokyo Institute of Technology, 2-12-1 O-okayama, Meguro, Tokyo 152-8551, Japan*

¹⁷*Department of Physics, Tohoku University, Sendai 980-8578, Japan*

¹⁸*Center for Nuclear Study, University of Tokyo, RIKEN campus, Wako, Saitama 351-0198, Japan*

¹⁹*Key Laboratory of Beam Technology and Material Modification of Ministry of Education,*

College of Nuclear Science and Technology, Beijing Normal University, Beijing 100875, People's Republic of China

²⁰*Cyclotron and Radioisotope Center, Tohoku University, Sendai 980-8578, Japan*

²¹*Department of Physics, Konan University, Kobe 658-8501, Japan*

²²*Department of Physics, University of Tokyo, 7-3-1 Hongo, Bunkyo, Tokyo 113-0033, Japan*

²³*Horia Hulubei National Institute for R&D in Physics and Nuclear Engineering, IFIN-HH, 077125 București-Măgurele, Romania*

²⁴*Doctoral School of Physics, University of Bucharest, 077125 București-Măgurele, Romania*

²⁵*Department of Physics, Rikkyo University, 3-34-1 Nishi-Ikebukuro, Toshima, Tokyo 172-8501, Japan*



(Received 8 January 2023; revised 17 March 2023; accepted 29 March 2023; published 27 April 2023)

We report on the first proton-induced single proton- and neutron-removal reactions from the neutron-deficient ^{14}O nucleus with large Fermi-surface asymmetry $S_n - S_p = 18.6$ MeV at ~ 100 MeV/nucleon, a widely used energy regime for rare-isotope studies. The measured inclusive cross sections and parallel momentum distributions of the ^{13}N and ^{13}O residues are compared to the state-of-the-art reaction models, with nuclear structure inputs from many-body shell-model calculations. Our results provide the first quantitative contributions of multiple reaction mechanisms including the quasifree knockout, inelastic scattering, and nucleon transfer processes. It is shown that the inelastic scattering and nucleon transfer, usually neglected at such energy regime, contribute about 50% and 30% to the loosely bound proton and deeply bound neutron removal, respectively. These multiple reaction mechanisms should be considered in analyses of inclusive one-nucleon removal cross sections measured at intermediate energies for quantitative investigation of single-particle strengths and correlations in atomic nuclei.

DOI: [10.1103/PhysRevLett.130.172501](https://doi.org/10.1103/PhysRevLett.130.172501)

Published by the American Physical Society under the terms of the [Creative Commons Attribution 4.0 International](https://creativecommons.org/licenses/by/4.0/) license. Further distribution of this work must maintain attribution to the author(s) and the published article's title, journal citation, and DOI.

The concept of independent particle motion has played a fundamental role for the study of quantum many-body systems, such as metallic clusters, atoms, and nuclei [1]. For the nuclear many-body systems, a first-order description was realized via the independent particle model [2–4], in which nucleons move freely in an effective mean-field potential provided by all the other nucleons. Nucleon-nucleon correlations should be added for a realistic description of nuclear properties. It was first revealed by $(e, e'p)$ experiments on stable nuclei that the nuclear single-particle strengths, quantified by the so-called spectroscopic factors, are reduced by (30–40)% relative to the independent particle model predictions [5,6]. The “quenching” of the single-particle strengths has been attributed to long-range [7,8] and short-range [9–12] correlations, whose investigations have significantly improved our understanding of the strongly correlated nuclear many-body system and led to new insights for dense nuclear matter such as neutron stars [13,14]. One main focus of today’s nuclear physics is to extend the correlation studies toward the proton and neutron driplines [15,16].

One-nucleon removal reactions at intermediate energies near and above 100 MeV/nucleon have been a powerful tool to extract single-particle strengths of unstable nuclei [17]. The quenching of the single-particle strengths has been connected to the so-called reduction factor R_s [18], defined as the ratio of the experimental to the theoretical cross section that is usually computed using shell-model spectroscopic factors and a reaction model relying on the adiabatic (or sudden) and eikonal approximations [17]. The central assumptions are that the residue and removed-nucleon relative motion is considered as frozen and the trajectories follow straight lines before and after the collision. Systematic studies from light-ion-induced one-nucleon removal reactions at ~ 100 MeV/nucleon [19–21] and higher incident beam energies [22] revealed that R_s has a strong dependence on the Fermi-surface asymmetry quantified as $\Delta S = S_n - S_p$ or $S_p - S_n$ for neutron or proton removal, respectively. However, results from transfer reactions [23–29] and proton-induced quasifree knockout (p, pN) reactions [30–34] did not confirm the strong ΔS dependence.

The inconsistent dependence on ΔS calls for a deeper understanding of reaction mechanisms and correlations in nuclei [16]. Although the diffraction and stripping mechanisms have been well-established in the eikonal model down to ~ 100 MeV/nucleon [35,36], multiple scattering, excitation, and decay of the one-nucleon removal residue, beyond the eikonal reaction model [37,38] or Pauli blocking [39,40], have been proposed as possible mechanisms that could reduce the deeply bound nucleon-removal cross sections. In particular, asymmetric parallel momentum distributions (PMDs) of the residue, characterized by a low-momentum tail [41–48] and a high-momentum

cutoff [45], have been observed in several experiments, in contrast to the symmetric PMDs predicted by the lowest order eikonal model [49–51].

Aforementioned studies [19–22] have been conducted with light absorptive nuclear targets, ^9Be or ^{12}C , which introduce the complexity that the final state of the target is unknown. Here, we report on the first study of one-nucleon removal from a large Fermi-surface asymmetric nucleus ^{14}O ($\Delta S = \pm 18.6$ MeV) at ~ 100 MeV/nucleon using a single-nucleon target, i.e., protons. ^{14}O is an ideal nucleus to study the one-nucleon removal mechanisms at large proton-to-neutron asymmetry. The proton and neutron removal from it involves only the orbitals of $\pi 0p_{1/2}$ and $\nu 0p_{3/2}$, respectively, since both ^{13}N ($J_{\text{g.s.}}^\pi = 1/2^-$) and ^{13}O ($J_{\text{g.s.}}^\pi = 3/2^-$) do not exhibit bound excited states. Based on the measured PMDs and the state-of-the-art reaction models, we show that in addition to the quasifree knockout, the inelastic scattering, and nucleon transfer also make significant contributions to the loosely bound proton removal and deeply bound neutron removal, respectively.

The experiment was performed at the Radioactive Isotope Beam Factory operated by the RIKEN Nishina Center and the Center for Nuclear Study, The University of Tokyo. A primary ^{18}O beam at 230 MeV/nucleon with an intensity of 500 pA bombarded on a 14-mm thick ^9Be target. The ^{14}O secondary beam was purified and identified using the time of flight (TOF) and the energy loss (ΔE) information by the BigRIPS fragment separator [52]. The typical ^{14}O beam intensity and purity were 9×10^3 particles per second and 78%, respectively. The ^{14}O beam was tracked onto a 2.40(34)-mm thick solid hydrogen target [53] using two multiwire drift chambers. The beam energy at the target center was 94 MeV/nucleon with a narrow spread of 0.2 MeV/nucleon (σ). The target density was determined to be 86 mg/cm³ based on the monitored target-cell temperature. The target thickness and its uncertainty were extracted by measuring the momentum change of the unreacted ^{14}O beam with and without the hydrogen target. The empty-target setting was also used to measure the background generated by nontarget beamline materials, which were subtracted in the cross section and PMD analyses.

The reaction residues were measured by the SAMURAI spectrometer [54], with a magnetic field set at 1.49 Tesla with filled target and 1.51 Tesla with empty target. Positions and angles of the particles were measured by two multiwire drift chambers located before and after the dipole magnet. A 10-mm thick plastic scintillator array hodoscope located downstream of the spectrometer was used to measure the ΔE and to determine the TOF together with a 0.2-mm thick plastic scintillator before the target. The magnetic rigidity $B\rho$ and the flight length from the target to hodoscope were deduced from multidimensional-fit functions using measured positions and angles as inputs.

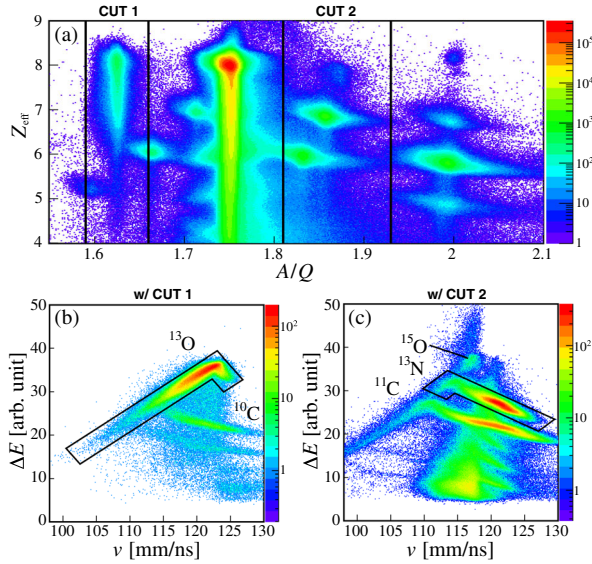


FIG. 1. Particle identification of projectilelike residues. Particle's velocity (ν) is deduced from TOF. Combining $B\rho$ and velocity allows to determine particle's mass-to-charge ratio A/Q . Z_{eff} is the deduced effective atomic number with ΔE and velocity using the Bethe-Bloch formula. The energy deposit of a charged particle in a material is related to its velocity, charge, and mass, as shown in the ΔE - ν spectra with (w/) the A/Q selections from 1.59 to 1.66 (b) and from 1.81 to 1.93 (c). Black contours in (b) and (c) select ^{13}O and ^{13}N , respectively.

The functions, obtained through Geant4 [55] simulations and multidimensional fit package of ROOT [56], reproduce the simulated $B\rho$ and flight length with relative deviations below 0.02%.

As shown in Fig. 1, ^{13}O and ^{13}N can be unambiguously identified using the ΔE - $B\rho$ -TOF and ΔE -velocity method. In Fig. 1(a), the deduced atomic number Z_{eff} for ^{13}O

($A/Q = 1.625$) and ^{14}O ($A/Q = 1.75$) both show tails extending to smaller Z_{eff} region. The Z_{eff} tail of ^{14}O is caused by unreacted ^{14}O projectiles interacting in the hodoscope, while the Z_{eff} tail of ^{13}O has a strong component steaming from the low-energy ^{13}O stopped in the hodoscope. As demonstrated in Figs. 1(b) and 1(c), most ^{13}O stopped in the hodoscope and had ΔE proportional to velocity, while most ^{13}N punched through the hodoscope and had ΔE antiproportional to velocity.

The resulting experimental cross sections are listed in Table I. Momentum acceptances, 94(1)% for ^{13}O and 96(1)% for ^{13}N , determined from Geant4 simulations and 7(1)% reaction loss in the beamline materials have been taken into account. In addition, a 5(1)% loss was considered to account for ^{13}O or ^{13}N events outside of the gates in Figs. 1(b) and 1(c), based on simulations with the Liège Intranuclear Cascade model [57], which is a well-established model for the description of spallation reactions. The cross section errors for ^{13}O and ^{13}N contain statistical uncertainties (0.6% and 1.3%), particle selections (0.9% and 2.3%), and systematic uncertainties (14.2% and 14.7%) mainly resulting from the target-thickness uncertainty. The experimental PMDs of ^{13}O and ^{13}N are shown in Fig. 2. An asymmetric PMD with a low-momentum tail and a high-momentum sharp edge is observed in the deeply bound neutron removal channel, while the PMD from the loosely bound proton removal is close to symmetric.

The experimental cross sections and PMDs were compared to predictions combining structure and reaction inputs. Spectroscopic factors for the removed nucleons were obtained from shell-model calculations. See Supplemental Material (SM) [58] for details. For the (p, pN) knockout process, we adopted the DWIA (Distorted-Wave Impulse Approximation) [74–78] and the QTC (Quantum Transfer-to-the-Continuum) [32,79]

TABLE I. Experimental (σ_{exp}) and theoretical (σ_{th}) cross sections for one-nucleon removal from ^{14}O at 94 MeV/nucleon. SF represents the spectroscopic factor from shell-model calculations (see SM [58]). The reduction factors $R_s = \sigma_{\text{exp}}/\sigma_{\text{th}}$ are also given.

Residue	J^π	σ_{exp} (mb)	SF	Theory	σ_{sp} (mb)	σ_{th} (mb)	R_s
$^{13}\text{N}_{\text{g.s.}}$	$1/2^-$	10.7(16)	1.58	DWIA	5.2	8.8	1.22(18)
				Inelastic	...	9	
				Sum		17.8	0.60(9)
				QTC	7.0	11.9	0.90(13)
				Inelastic Sum	...	9	20.9
$^{13}\text{O}_{\text{g.s.}}$	$3/2^-$	16.7(24)	3.42	DWIA	6.3	23.2	0.72(10)
				Transfer	3	11	
				Sum		34.2	0.49(7)
				QTC	10.2	37.6	0.44(6)
				w/o transfer QTC	13.5	49.7	0.34(5)

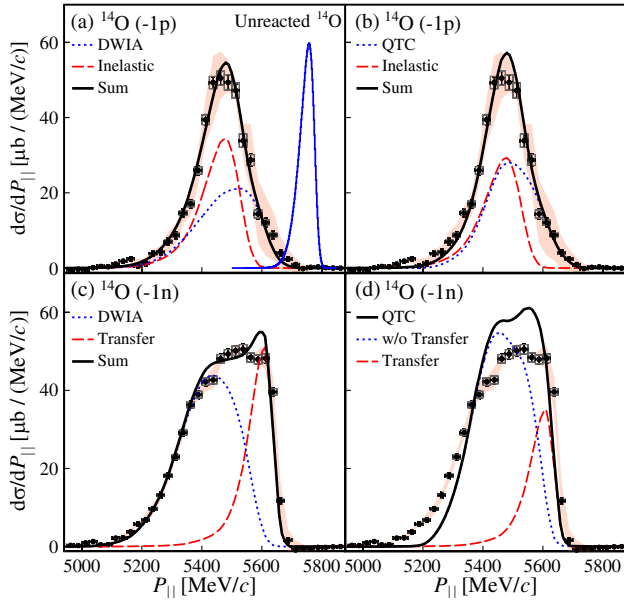


FIG. 2. Parallel momentum distributions of ^{13}N and ^{13}O . The black-filled markers show the experimental data. The orange bands represent the uncertainties from the background subtractions. The gray empty bins indicate the other systematic uncertainties. Panels (a)–(c) compare the data to DWIA and QTC calculations (blue dotted lines), with additional contributions from inelastic excitation for ^{13}N and (p, d) transfer for ^{13}O (red dashed lines). Panel (d) displays the QTC calculation as a black solid line, while the calculation without (w/o) (p, d) transfer is represented by a blue dotted line. The blue solid line in (a) shows the distribution of the unreacted ^{14}O beam (shifted by -200 MeV/c) to demonstrate the experimental response, which introduces a shift and broadening of the momentum due to energy losses and detector resolutions. Theoretical distributions have been convoluted with the experimental response and their integrals have been normalized to the experimental cross sections, without any momentum shift to match the data. Note that the sharp (p, d) transfer peak is smoothed out by the experimental response. See SM [58] for theoretical distributions before experimental response convolution.

models (see SM [58]). Both models assume a single scattering between the removed nucleon and the target proton, using the transition amplitude to calculate the cross sections. The key disparity lies in how they handle the three-body final state: DWIA factorizes it as the product of the p -residue and N -residue states, while QTC expands it in terms of p - N states, including deuteron ground state for neutron removal [78]. The DWIA and QTC reaction models have been developed and benchmarked for (p, pN) reactions at beam energies higher than 200 MeV/nucleon [32,78]. Above 200 MeV/nucleon, both models reproduce well the shape of the experimental momentum distributions [32,80–82], and the calculated single-particle cross sections (σ_{sp}) are consistent with each other within 20% [83]. The obtained σ_{sp} for $^{14}\text{O}(p, 2p)^{13}\text{N}$ and $^{14}\text{O}(p, pn)^{13}\text{O}$ reactions are listed in Table I.

In addition, we also considered the (p, p') inelastic excitation of ^{14}O to its low-lying excited states located above S_p and below $\sim S_{2p}$, which decay to the ground state of ^{13}N via one-proton emission. Giant-resonance excitations were not considered. A total inelastic cross section of 9 mb was obtained (see SM [58]). As shown in Figs. 2(a) and 2(b), the sum of the $(p, 2p)$ and (p, p') PMDs is close to symmetric and reproduces well the PMD of ^{13}N . The good agreement confirms the predicted strong inelastic-scattering component in the loosely bound proton removal, which has fractional contributions of 51% with the DWIA and of 43% with the QTC. The inelastic-scattering component was also observed in the one-nucleon removal with a ^9Be target using the invariant-mass technique [48,59]. Percentage contributions of 17% and 21% from the inelastic scattering were extracted for the one-proton removal from ^9C and ^{13}O at ~ 65 MeV/nucleon [48]. If the inelastic-scattering component is ignored, the present one-proton removal R_s will be around unity, coinciding with the loosely bound nucleon-removal R_s from eikonal model based analysis [19–21,35]. Performing additional coincidence measurements with the recoil and decayed protons to obtain the angular distribution and the ^{14}O excitation energy would further characterize the inelastic components. The low-lying excited states considered here have multiparticle-multihole configurations. It was shown recently that inelastic scattering with large momentum transfer has the advantage of populating multiparticle-multihole states [84]. Descriptions of such states are beyond the (p, pN) and the eikonal models, which assume beforehand that the projectile is a single-particle state plus an inert core [17].

For the deeply bound neutron removal, the (p, d) transfer is considered in the QTC formalism but not in the DWIA. To study the (p, d) transfer effect, we performed the QTC calculation with the outgoing channel coupled only to the deuteron ground state, that is equivalent to the so-called DWBA (Distorted-Wave Born Approximation) calculation. The obtained σ_{sp} for the transfer reaction is 3 mb with an uncertainty of about 1 mb (see SM [58]). The QTC σ_{sp} without the (p, d) transfer is still larger than the DWIA result. Other effects, such as low-energy neutron-core absorption, contribute to this difference.

As shown in Fig. 2(c), the PMD of ^{13}O is well reproduced by combining the contributions from the DWIA and the DWBA, in which the latter corresponding to (p, d) transfer contributes to $\sim 30\%$. Our data supports the interpretation of Ref. [76] that the low-momentum tail is caused by the attractive potential between the outgoing nucleons and ^{13}O . Meanwhile, the (p, d) transfer reaction creates a sharp high-momentum edge, as observed in the data, due to the two-body kinematics of the transfer reaction. The sharp edge is found in a kinematic region

inaccessible to (p, pn) knockout and is thus a proof of the significant transfer contribution. Note that the sharp edge here has a different origin with that observed in Ref. [45], which is due to a threshold effect when the incident energy per particle is comparable to the nucleon separation energy. Additional characterization of the transfer contribution would be to measure the angular distribution of cross sections in coincidence with the deuteron. See for example Ref. [85]. Since QTC formalism treats (p, d) transfer consistently with (p, pn) , it reproduces better the sharp high-momentum side than DWIA, as shown in Fig. 2(d). However, QTC does not reproduce the low-momentum tail as well as DWIA. The reason might be due to the different treatment of the final state interaction in QTC, especially that the nucleon-residue interaction at low relative energy is not explicitly treated in QTC formalism.

It is the first time the PMD measured near 100 MeV/nucleon shows a distinctive contribution from the (p, d) transfer reaction, usually neglected at such beam energies [16]. One-nucleon pickup cross sections have been measured around 60 MeV/nucleon with heavy-ion beams on ^{12}C or ^9Be target [86–89]. Here, the extracted one-neutron transfer cross section is higher due to the momentum matching of the well-bound neutron. The product of the momentum transfer q and the radius of ^{14}O nucleus R is around $(1-2)\hbar$ at forward angles, which fits the momentum matching condition [26,90]. Further calculations at 300 MeV/nucleon show the qR product increases to $(3-5)\hbar$ and the (p, d) transfer cross section decreases to about 0.2 mb, negligible compared to the quasifree knockout cross sections [31,51]. The transfer contribution should thus be assessed for one-nucleon removal reactions at intermediate energies, especially at energies below 100 MeV/nucleon. We infer that the one-nucleon removal with a nuclear target may also contain non-negligible transfer contributions, where the removed nucleon combines with the target nucleus forming bound or resonance states, depending on the energy and angular momentum matching.

R_s as a function of ΔS is shown in Fig. 3. Most light-ion-induced nucleon removal R_s lie within a band with a slope of $-1.6 \times 10^{-2} \text{ MeV}^{-1}$ and a half width of 0.1 [19–21], as shown by the shaded gray region. Contrastingly, analyses of low-energy one-nucleon transfer [25,27,28,91] and high-energy quasifree scattering data [30–32,34] give slope absolute values of $(10^{-3}-10^{-5}) \text{ MeV}^{-1}$. By considering the two datasets of the present work, we obtain a slope of $-3.0(5)(5) \times 10^{-3} \text{ MeV}^{-1}$ when the DWIA together with the inelastic and transfer calculations are considered, and of $-4.6(4)(7) \times 10^{-3} \text{ MeV}^{-1}$ when the QTC and the inelastic scattering are considered. Both slopes are negative and their absolute values are almost zero, indicating R_s have a weak ΔS dependence. For comparison, we also extract the R_s if the inelastic scattering and nucleon transfer are neglected in cross-section calculations. The resulting R_s slopes in the

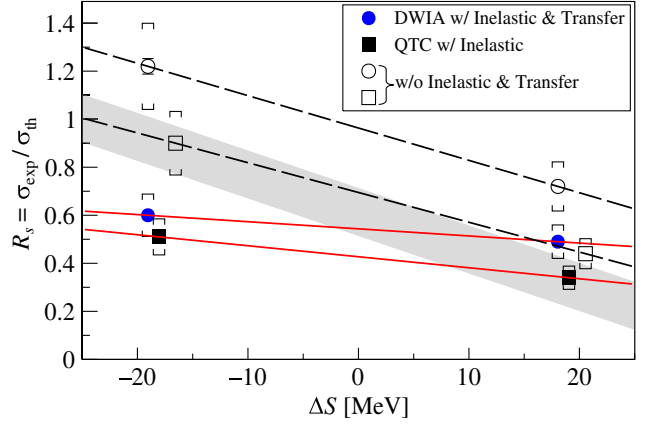


FIG. 3. R_s as a function of ΔS from the present work (blue dots and black squares) compared to the trend extracted from Be or C induced nucleon-removal cross sections analyzed with the eikonal model [19–21] (gray shaded region). The square brackets indicate the total systematic uncertainties. Red solid and black dashed lines are shown to guide the eyes.

absolute values are 3–5 times larger and look compatible with the strong ΔS dependence indicated by the light-ion-induced nucleon removal.

In summary, we have reported on the first study of the one-nucleon removal reactions from a large Fermi-surface asymmetric nucleus ^{14}O ($\Delta S = \pm 18.6 \text{ MeV}$) using a proton target at $\sim 100 \text{ MeV/nucleon}$, a widely used energy regime for rare-isotope studies. The measured cross sections and PMDs were compared to the state-of-the-art reaction models, including quasifree knockout, inelastic scattering, and nucleon transfer calculations. In the loosely bound proton removal channel, the (p, p') inelastic scattering and the $(p, 2p)$ quasifree knockout are found of almost equal contributions, advocating for an explicit treatment of the inelastic scattering for quantitative interpretation of loosely bound nucleon-removal cross sections. A highly asymmetric PMD was observed in the deeply bound neutron-removal channel, which was reproduced by combining the (p, pn) knockout component from DWIA calculations and the (p, d) transfer component from DWBA calculations. We observed a distinctive contribution of $\sim 30\%$ in the high-momentum part of the residue PMD from the deeply bound nucleon stripping (p, d) transfer reaction, usually not considered at such beam energies. The reduction factors extracted from the present two new datasets show a weak ΔS dependence, which is at tension with the eikonal analysis of light-ion-induced knockout reactions. The extracted dependence becomes markedly steeper if the inelastic scattering and nucleon transfer contributions are ignored, suggesting that these processes should be considered in analyses of inclusive one-nucleon removal cross sections measured at intermediate energies for quantitative investigation of single-particle strengths and correlations in atomic nuclei.

We are grateful to the RIKEN Nishina Center accelerator staff for providing the stable and high-intensity ^{18}O beam and to the BigRIPS team for the smooth operation of the secondary beam. This work was supported by the Deutsche Forschungsgemeinschaft (DFG, German Research Foundation)–Projektnummer 279384907–SFB 1245. Y. L. S. and A. O. acknowledge the support from the Alexander von Humboldt foundation. Y. L. S. acknowledges the support of Marie Skłodowska-Curie Individual Fellowship (H2020-MSCA-IF-2015-705023) from the European Union and the support from the Helmholtz International Center for FAIR. K. O. acknowledges the support by Grant-in-Aid for Scientific Research JP21H00125. M. G. R. acknowledges financial support by MCIN/AEI/10.13039/501100011033 under I + D + i project No. PID2020–114687 GB-I00, by the Consejería de Economía, Conocimiento, Empresas y Universidad, Junta de Andalucía (Spain) and “ERDF-A Way of Making Europe” under PAIDI 2020 project No. P20_01247, and by the European Social Fund and Junta de Andalucía (PAIDI 2020) under grant no. DOC-01006. C. X. Y. acknowledges Guangdong Major Project of Basic and Applied Basic Research (2021B0301030006). J. L. acknowledges the support from Research Grants Council (RGC) of Hong Kong (GRF-17303717). T. N. acknowledges the JSPS Kakenhi Grants No. JP16H02179, JP18H05404. Y. T. acknowledges the JSPS Grant-in-Aid for Scientific Research Grants No. JP21H01114. H. N. L. acknowledges the Fundamental Research Funds for the Central Universities of China. This work was supported by the Institute for Basic Science (IBS-R031-D1). B. A. B. was supported by NSF Grant No. PHY-2110365. Y. Satou is thanked for his help with the inelastic scattering calculations. We thank T. Aumann, C. A. Bertulani, and M. Duer for their valuable comments on the manuscript.

*Corresponding author.

ysun@ikp.tu-darmstadt.de

- [1] V. R. Pandharipande, I. Sick, and P. K. A. d. Huberts, *Rev. Mod. Phys.* **69**, 981 (1997).
- [2] M. G. Mayer, *Phys. Rev.* **75**, 1969 (1949).
- [3] O. Haxel, J. H. D. Jensen, and H. E. Suess, *Phys. Rev.* **75**, 1766 (1949).
- [4] A. Bohr and B. R. Mottleson, *Nuclear Structure* (Benjamin, New York, 1969), Vol. I.
- [5] L. Lapikás, *Nucl. Phys.* **A553**, 297 (1993).
- [6] G. Kramer, H. Blok, and L. Lapikás, *Nucl. Phys.* **A679**, 267 (2001).
- [7] W. Dickhoff and C. Barbieri, *Prog. Part. Nucl. Phys.* **52**, 377 (2004).
- [8] C. Barbieri, *Phys. Rev. Lett.* **103**, 202502 (2009).
- [9] E. Piasezky, M. Sargsian, L. Frankfurt, M. Strikman, and J. W. Watson, *Phys. Rev. Lett.* **97**, 162504 (2006).
- [10] R. Subedi, R. Shneor, P. Monaghan, B. Anderson, K. Aniol, J. Annand, J. Arrington, H. Benaoum, F. Benmokhtar, W. Bertozzi *et al.*, *Science* **320**, 1476 (2008).
- [11] O. Hen, M. Sargsian, L. B. Weinstein, E. Piasezky, H. Hakobyan, D. W. Higinbotham, M. Braverman, W. K. Brooks, S. Gilad, K. P. Adhikari *et al.*, *Science* **346**, 614 (2014).
- [12] M. Duer, O. Hen, E. Piasezky, H. Hakobyan, L. B. Weinstein, M. Braverman, E. O. Cohen, D. Higinbotham, K. P. Adhikari, S. Adhikari *et al.*, *Nature (London)* **560**, 617 (2018).
- [13] D. Ding, A. Rios, H. Dussan, W. H. Dickhoff, S. J. Witte, A. Carbone, and A. Polls, *Phys. Rev. C* **94**, 025802 (2016).
- [14] N. Fomin, D. Higinbotham, M. Sargsian, and P. Solvignon, *Annu. Rev. Nucl. Part. Sci.* **67**, 129 (2017).
- [15] S. Paschalis, M. Petri, A. Macchiavelli, O. Hen, and E. Piasezky, *Phys. Lett. B* **800**, 135110 (2020).
- [16] T. Aumann, C. Barbieri, D. Bazin, C. Bertulani, A. Bonaccorso, W. Dickhoff, A. Gade, M. Gómez-Ramos, B. Kay, A. Moro *et al.*, *Prog. Part. Nucl. Phys.* **118**, 103847 (2021).
- [17] P. Hansen and J. Tostevin, *Annu. Rev. Nucl. Part. Sci.* **53**, 219 (2003).
- [18] B. A. Brown, P. G. Hansen, B. M. Sherrill, and J. A. Tostevin, *Phys. Rev. C* **65**, 061601(R) (2002).
- [19] A. Gade, P. Adrich, D. Bazin, M. D. Bowen, B. A. Brown, C. M. Campbell, J. M. Cook, T. Glasmacher, P. G. Hansen, K. Hosier *et al.*, *Phys. Rev. C* **77**, 044306 (2008).
- [20] J. A. Tostevin and A. Gade, *Phys. Rev. C* **90**, 057602 (2014).
- [21] J. A. Tostevin and A. Gade, *Phys. Rev. C* **103**, 054610 (2021).
- [22] Y. Z. Sun, S. T. Wang, Y. P. Xu, D. Y. Pang, J. G. Li, C. X. Yuan, L. F. Wan, Y. Qiao, Y. Q. Wang, and X. Y. Chen, *Phys. Rev. C* **106**, 034614 (2022).
- [23] J. Lee, J. A. Tostevin, B. A. Brown, F. Delaunay, W. G. Lynch, M. J. Saelim, and M. B. Tsang, *Phys. Rev. C* **73**, 044608 (2006).
- [24] J. Lee, M. B. Tsang, D. Bazin, D. Coupland, V. Henzl, D. Henzlova, M. Kilburn, W. G. Lynch, A. M. Rogers, A. Sanetullaev *et al.*, *Phys. Rev. Lett.* **104**, 112701 (2010).
- [25] F. Flavigny, A. Gillibert, L. Nalpas, A. Obertelli, N. Keeley, C. Barbieri, D. Beaumel, S. Boissinot, G. Burgunder, A. Cipollone *et al.*, *Phys. Rev. Lett.* **110**, 122503 (2013).
- [26] B. P. Kay, J. P. Schiffer, and S. J. Freeman, *Phys. Rev. Lett.* **111**, 042502 (2013).
- [27] Y. Xu, D. Pang, X. Yun, C. Wen, C. Yuan, and J. Lou, *Phys. Lett. B* **790**, 308 (2019).
- [28] J. Manfredi, J. Lee, A. M. Rogers, M. B. Tsang, W. G. Lynch, C. Anderson, J. Barney, K. W. Brown, B. Brophy, G. Cerizza *et al.*, *Phys. Rev. C* **104**, 024608 (2021).
- [29] B. P. Kay, T. L. Tang, I. A. Tolstukhin, G. B. Roderick, A. J. Mitchell, Y. Ayyad, S. A. Bennett, J. Chen, K. A. Chippis, H. L. Crawford *et al.*, *Phys. Rev. Lett.* **129**, 152501 (2022).
- [30] S. Kawase, T. Uesaka, T. L. Tang, D. Beaumel, M. Dozono, T. Fukunaga, T. Fujii, N. Fukuda, A. Galindo-Uribarri, S. Hwang *et al.*, *Prog. Theor. Exp. Phys.* **2018** (2018).
- [31] L. Atar, S. Paschalis, C. Barbieri, C. A. Bertulani, P. Díaz Fernández, M. Holl, M. A. Najafi, V. Panin, H. Alvarez-Pol, T. Aumann *et al.* (R^3B Collaboration), *Phys. Rev. Lett.* **120**, 052501 (2018).

- [32] M. Gómez-Ramos and A. Moro, *Phys. Lett. B* **785**, 511 (2018).
- [33] M. Holl, V. Panin, H. Alvarez-Pol, L. Atar, T. Aumann, S. Beceiro-Novo, J. Benlliure, C. Bertulani, J. Boillos, K. Boretzky *et al.*, *Phys. Lett. B* **795**, 682 (2019).
- [34] Nguyen Tri Toan Phuc, K. Yoshida, and K. Ogata, *Phys. Rev. C* **100**, 064604 (2019).
- [35] D. Bazin, R. J. Charity, R. T. de Souza, M. A. Famiano, A. Gade, V. Henzl, D. Henzlova, S. Hudan, J. Lee, S. Lukyanov *et al.*, *Phys. Rev. Lett.* **102**, 232501 (2009).
- [36] K. Wimmer, D. Bazin, A. Gade, J. A. Tostevin, T. Baugher, Z. Chajecski, D. Coupland, M. A. Famiano, T. K. Ghosh, G. F. Grinyer *et al.*, *Phys. Rev. C* **90**, 064615 (2014).
- [37] C. Louchart, A. Obertelli, A. Boudard, and F. Flavigny, *Phys. Rev. C* **83**, 011601(R) (2011).
- [38] Y. L. Sun, J. Lee, Y. L. Ye, A. Obertelli, Z. H. Li, N. Aoi, H. J. Ong, Y. Ayyad, C. A. Bertulani, J. Chen *et al.*, *Phys. Rev. C* **93**, 044607 (2016).
- [39] F. Flavigny, A. Obertelli, and I. Vidaña, *Phys. Rev. C* **79**, 064617 (2009).
- [40] C. A. Bertulani and C. De Conti, *Phys. Rev. C* **81**, 064603 (2010).
- [41] J. A. Tostevin, D. Bazin, B. A. Brown, T. Glasmacher, P. G. Hansen, V. Maddalena, A. Navin, and B. M. Sherrill, *Phys. Rev. C* **66**, 024607 (2002).
- [42] A. Gade, D. Bazin, C. A. Bertulani, B. A. Brown, C. M. Campbell, J. A. Church, D. C. Dinca, J. Enders, T. Glasmacher, P. G. Hansen *et al.*, *Phys. Rev. C* **71**, 051301(R) (2005).
- [43] K. L. Yurkewicz, D. Bazin, B. A. Brown, J. Enders, A. Gade, T. Glasmacher, P. G. Hansen, V. Maddalena, A. Navin, B. M. Sherrill *et al.*, *Phys. Rev. C* **74**, 024304 (2006).
- [44] G. F. Grinyer, D. Bazin, A. Gade, J. A. Tostevin, P. Adrich, M. D. Bowen, B. A. Brown, C. M. Campbell, J. M. Cook, T. Glasmacher *et al.*, *Phys. Rev. Lett.* **106**, 162502 (2011).
- [45] F. Flavigny, A. Obertelli, A. Bonaccorso, G. F. Grinyer, C. Louchart, L. Nalpas, and A. Signoracci, *Phys. Rev. Lett.* **108**, 252501 (2012).
- [46] R. Shane, R. J. Charity, L. G. Sobotka, D. Bazin, B. A. Brown, A. Gade, G. F. Grinyer, S. McDaniel, A. Ratkiewicz, D. Weisshaar *et al.*, *Phys. Rev. C* **85**, 064612 (2012).
- [47] S. R. Stroberg, A. Gade, J. A. Tostevin, V. M. Bader, T. Baugher, D. Bazin, J. S. Berryman, B. A. Brown, C. M. Campbell, K. W. Kemper *et al.*, *Phys. Rev. C* **90**, 034301 (2014).
- [48] R. J. Charity, L. G. Sobotka, and J. A. Tostevin, *Phys. Rev. C* **102**, 044614 (2020).
- [49] C. A. Bertulani and K. W. McVoy, *Phys. Rev. C* **46**, 2638 (1992).
- [50] J. Tostevin, *Nucl. Phys.* **A682**, 320 (2001).
- [51] T. Aumann, C. A. Bertulani, and J. Ryckebusch, *Phys. Rev. C* **88**, 064610 (2013).
- [52] N. Fukuda, T. Kubo, T. Ohnishi, N. Inabe, H. Takeda, D. Kameda, and H. Suzuki, *Nucl. Instrum. Methods Phys. Res., Sect. B* **317**, 323 (2013).
- [53] Y. Matsuda, H. Sakaguchi, J. Zenihiro, S. Ishimoto, S. Suzuki, H. Otsu, T. Ohnishi, H. Takeda, K. Ozeki, K. Tanaka *et al.*, *Nucl. Instrum. Methods Phys. Res., Sect. A* **643**, 6 (2011).
- [54] T. Kobayashi, N. Chiga, T. Isobe, Y. Kondo, T. Kubo, K. Kusaka, T. Motobayashi, T. Nakamura, J. Ohnishi, H. Okuno *et al.*, *Nucl. Instrum. Methods Phys. Res., Sect. B* **317**, 294 (2013).
- [55] S. Agostinelli, J. Allison, K. Amako, J. Apostolakis, H. Araujo, P. Arce, M. Asai, D. Axen, S. Banerjee, G. Barrand *et al.*, *Nucl. Instrum. Methods Phys. Res., Sect. A* **506**, 250 (2003).
- [56] R. Brun and F. Rademakers, *Nucl. Instrum. Methods Phys. Res., Sect. A* **389**, 81 (1997).
- [57] A. Boudard, J. Cugnon, S. Leray, and C. Volant, *Phys. Rev. C* **66**, 044615 (2002).
- [58] See Supplemental Material at <http://link.aps.org/supplemental/10.1103/PhysRevLett.130.172501> for more details of shell model calculations as well as DWIA, QTC, and the inelastic excitation calculations, which includes Refs. [59–73].
- [59] R. J. Charity, K. W. Brown, J. Okołowicz, M. Płoszajczak, J. M. Elson, W. Reviol, L. G. Sobotka, W. W. Buhro, Z. Chajecski, W. G. Lynch *et al.*, *Phys. Rev. C* **100**, 064305 (2019).
- [60] M. A. Franey and W. G. Love, *Phys. Rev. C* **31**, 488 (1985).
- [61] F. Perey and B. Buck, *Nucl. Phys.* **32**, 353 (1962).
- [62] J.-P. Jeukenne, A. Lejeune, and C. Mahaux, *Phys. Rev. C* **16**, 80 (1977).
- [63] R. C. Johnson and P. J. R. Soper, *Phys. Rev. C* **1**, 976 (1970).
- [64] V. G. J. Stoks, R. A. M. Klomp, C. P. F. Terheggen, and J. J. de Swart, *Phys. Rev. C* **49**, 2950 (1994).
- [65] R. Schaeffer and J. Raynal, computer program DWBA70, 1970 (unpublished); extended version DW81 by J. R. Comfort, 1981 (unpublished).
- [66] A. Koning and J. Delaroche, *Nucl. Phys.* **A713**, 231 (2003).
- [67] J. R. Comfort, G. L. Moake, C. C. Foster, P. Schwandt, C. D. Goodman, J. Rapaport, and W. G. Love, *Phys. Rev. C* **24**, 1834 (1981).
- [68] G. Bertsch, J. Borysowicz, H. McManus, and W. Love, *Nucl. Phys.* **A284**, 399 (1977).
- [69] C. Yuan, T. Suzuki, T. Otsuka, F. Xu, and N. Tsunoda, *Phys. Rev. C* **85**, 064324 (2012).
- [70] N. Shimizu, T. Mizusaki, Y. Utsuno, and Y. Tsunoda, *Comput. Phys. Commun.* **244**, 372 (2019).
- [71] B. A. Brown, A. Etchegoyen, N. S. Godwin, W. D. M. Rae, W. A. Richter, W. E. Ormand, E. K. Warburton, J. S. Winfield, L. Zhao, C. H. Zimmerman *et al.*, MSU-NSCL report no. 1289, 2004.
- [72] E. K. Warburton and B. A. Brown, *Phys. Rev. C* **46**, 923 (1992).
- [73] A. E. L. Dieperink and T. d. Forest, *Phys. Rev. C* **10**, 543 (1974).
- [74] N. S. Chant and P. G. Roos, *Phys. Rev. C* **15**, 57 (1977).
- [75] N. S. Chant and P. G. Roos, *Phys. Rev. C* **27**, 1060 (1983).
- [76] K. Ogata, K. Yoshida, and K. Minomo, *Phys. Rev. C* **92**, 034616 (2015).
- [77] T. Wakasa, K. Ogata, and T. Noro, *Prog. Part. Nucl. Phys.* **96**, 32 (2017).
- [78] K. Yoshida, M. Gómez-Ramos, K. Ogata, and A. M. Moro, *Phys. Rev. C* **97**, 024608 (2018).

- [79] A. M. Moro, *Phys. Rev. C* **92**, 044605 (2015).
- [80] Y. Sun, A. Obertelli, P. Doornenbal, C. Barbieri, Y. Chazono, T. Duguet, H. Liu, P. Navrátil, F. Nowacki, K. Ogata *et al.*, *Phys. Lett. B* **802**, 135215 (2020).
- [81] S. Chen, J. Lee, P. Doornenbal, A. Obertelli, C. Barbieri, Y. Chazono, P. Navrátil, K. Ogata, T. Otsuka, F. Raimondi *et al.*, *Phys. Rev. Lett.* **123**, 142501 (2019).
- [82] F. Browne, S. Chen, P. Doornenbal, A. Obertelli, K. Ogata, Y. Utsuno, K. Yoshida, N. L. Achouri, H. Baba, D. Calvet *et al.*, *Phys. Rev. Lett.* **126**, 252501 (2021).
- [83] T. Aumann, C. Barbieri, D. Bazin, C. A. B. and A. Bonaccorso, W. H. Dickhoff, A. Gade, M. Gómez-Ramos, B. P. Kay, A. M. Moro, T. Nakamura *et al.*, *Prog. Part. Nucl. Phys.* **118**, 103847 (2021).
- [84] A. Gade, B. A. Brown, D. Weisshaar, D. Bazin, K. W. Brown, R. J. Charity, P. Farris, A. M. Hill, J. Li, B. Longfellow *et al.*, *Phys. Rev. Lett.* **129**, 242501 (2022).
- [85] J. Kasagi, G. M. Crawley, E. Kashy, J. Duffy, S. Gales, E. Gerlic, and D. Friesel, *Phys. Rev. C* **28**, 1065 (1983).
- [86] A. Gade, P. Adrich, D. Bazin, M. D. Bowen, B. A. Brown, C. M. Campbell, J. M. Cook, T. Glasmacher, K. Hosier, S. McDaniel *et al.*, *Phys. Rev. C* **76**, 061302(R) (2007).
- [87] S. McDaniel, A. Gade, J. A. Tostevin, T. Baugher, D. Bazin, B. A. Brown, J. M. Cook, T. Glasmacher, G. F. Grinyer, A. Ratkiewicz *et al.*, *Phys. Rev. C* **85**, 014610 (2012).
- [88] A. Gade, J. A. Tostevin, V. Bader, T. Baugher, D. Bazin, J. S. Berryman, B. A. Brown, D. J. Hartley, E. Lunderberg, F. Recchia *et al.*, *Phys. Rev. C* **93**, 031601(R) (2016).
- [89] A. Gade, J. A. Tostevin, V. Bader, T. Baugher, D. Bazin, J. S. Berryman, B. A. Brown, C. A. Diget, T. Glasmacher, D. J. Hartley *et al.*, *Phys. Rev. C* **93**, 054315 (2016).
- [90] D. Brink, *Phys. Lett.* **40B**, 37 (1972).
- [91] J. Lee, M. B. Tsang, and W. G. Lynch, *Phys. Rev. C* **75**, 064320 (2007).